International Journal of Nanomedicine

Dovepress
open access to scientific and medical research

Open Access Full Text Article

ORIGINAL RESEARCH

Preparation and controlled-release studies of a protocatechuic acid-magnesium/aluminum-layered double hydroxide nanocomposite

This article was published in the following Dove Press journal:
International Journal of Nanomedicine
17 May 2013
Number of times this article has been viewed

Farahnaz Barahuie[1]
Mohd Zobir Hussein[1]
Samer Hasan Hussein-Al-Ali[2]
Palanisamy Arulselvan[3]
Sharida Fakurazi[3,4]
Zulkarnain Zainal[1]

[1]Materials Synthesis and Characterization Laboratory, Institute of Advanced Technology (ITMA), [2]Laboratory of Molecular Biomedicine, Institute of Bioscience, [3]Laboratory of Vaccines and Immunotherapeutics, Institute of Bioscience, [4]Department of Human Anatomy, Faculty of Medicine and Health Sciences, Universiti Putra Malaysia, Serdang, Malaysia

Abstract: In the study reported here, magnesium/aluminum (Mg/Al)-layered double hydroxide (LDH) was intercalated with an anticancer drug, protocatechuic acid, using ion-exchange and direct coprecipitation methods, with the resultant products labeled according to the method used to produce them: "PANE" (ie, protocatechuic acid-Mg/Al nanocomposite synthesized using the ion-exchange method) and "PAND" (ie, protocatechuic acid-Mg/Al nanocomposite synthesized using the direct method), respectively. Powder X-ray diffraction and Fourier transform infrared spectroscopy confirmed the intercalation of protocatechuic acid into the inter-galleries of Mg/Al-LDH. The protocatechuic acid between the interlayers of PANE and PAND was found to be a monolayer, with an angle from the z-axis of 8° for PANE and 15° for PAND. Thermogravimetric and differential thermogravimetric analysis results revealed that the thermal stability of protocatechuic acid was markedly enhanced upon intercalation. The loading of protocatechuic acid in PANE and PAND was estimated to be about 24.5% and 27.5% (w/w), respectively. The in vitro release study of protocatechuic acid from PANE and PAND in phosphate-buffered saline at pH 7.4, 5.3, and 4.8 revealed that the nanocomposites had a sustained release property. After 72 hours incubation of PANE and PAND with MCF-7 human breast cancer and HeLa human cervical cancer cell lines, it was found that the nanocomposites had suppressed the growth of these cancer cells, with a half maximal inhibitory concentration of 35.6 μg/mL for PANE and 36.0 μg/mL for PAND for MCF-7 cells, and 19.8 μg/mL for PANE and 30.3 μg/mL for PAND for HeLa cells. No half maximal inhibitory concentration for either nanocomposite was found for 3T3 cells.

Keywords: Mg/Al-LDH, direct coprecipitation method, ion-exchange method, MCF-7, HeLa, 3T3

Introduction

One of the most prolific scientific advancements of the past few decades has been the birth of nanotechnology, which has provided new opportunities for producing materials with markedly varied and unusual properties that have huge potential in many fields such as optics, medical science, catalysis and agriculture.[1]

Searching for a safe and effective method of delivering bioactive molecules and drugs, especially anticancer drugs, to specific cells is an interesting and intriguing area of research in modern pharmaceutics.[2] Conventional drug therapy in cancer does not always provide the desired therapeutic effects because the drugs have limited aqueous solubility, resistance to treatment of cancer diseases, and degrade enzymatically. Moreover, high doses of these drugs are needed that can lead to severe side effects and are not cost-effective.[3]

Correspondence: Mohd Zobir Hussein
Materials Synthesis and Characterization Laboratory (MSCL), Institute of Advanced Technology (ITMA),
Universiti Putra Malaysia, Serdang, Selangor 43400, Malaysia
Tel +60 3 8946 8092
Fax +60 3 8946 8470
Email mzobir@putra.upm.edu.my

Layered double hydroxides (LDHs) are used extensively in medicine as a unique delivery carrier for genes and drugs due to their outstanding properties that make them suitable for delivering to cells. These properties include their good biocompatibility (eg, use as an antacid and anti-peptic agent);[4,5] less toxic effects compared with other inorganic nanoparticles;[6,7] high specific surface areas and chemical stability, which have resulted from functionalization and modification of their internal and external surfaces;[8,9] ability to offer loaded drugs full protection;[10] cell targeting abilities;[11,12] and ability to be used as controlled-release drug-delivery systems.[13]

LDHs, also known as "hydrotalcite-like compounds," are a class of anionic clays. Their structure is based on positively charged brucite-like layers containing hydroxides of metal cations M^{2+} and M^{3+}. The general formula of an LDH is:

$$\left[M^{2+}_{1-x}M^{3+}_{x}(OH)_2\right]^{X+}(A^{m-})_{x/m}\cdot nH_2O,$$

where "M^{2+}" and "M^{3+}" are divalent and trivalent metal cations, respectively, "A^{m-}" refers to an interlayer anion with an m charge, *n* is the number of water molecules in the interlayer space, and *x* is the layer charge density.[14]

Owing to the efficient drug-delivery feature of LDH nanocarriers, many pharmaceutically active compounds have been successfully intercalated into the interlayer gallery of LDH. Among them are the cardiovascular drugs fluvastatin and pravastatin;[15] anti-inflammatory drugs such as diclofenac[16] and fenbufen;[17] antihypertensive drugs like perindopril erbumine;[18,19] the antihistamine drug cetirizine hydrochloric acid;[20] and anticancer drugs such as cordycepin, which was intercalated into the gallery of magnesium/aluminum (Mg/Al)-LDH. It was observed that the resulting nanohybrid had greater stability and a greater suppression effect on U937 cancer cell growth than free cordecypin[3] and methotrexate (MTX). A MTX-Mg/Al nanohybrid had a much stronger inhibition effect on the proliferation of human MNNG-HOS osteosarcoma cancer cells compared with unbound MTX.[1]

Various methods have been used to intercalate drugs as guest molecules into LDHs, but the most common methods are direct coprecipitation and ion exchange.[21] Compared with the ion-exchange method, the direct coprecipitation method produces a large quantity of the nanocomposite and there is more risk with this method of carbon dioxide uptake and the incorporation of unwanted hydroxide anions in the reaction mixture.[22,23]

Protocatechuic acid (3,4-dihydroxybenzoic acid) is a natural phenolic acid isolated from a number of popular medicinal plants such as Sudan mallow (*Hibiscus sabdariffa* L.),[24,25] St John's wort (*Hypericum perforatum* L.),[26] and Japanese ginkgo (*Ginkgo biloba* L.).[27] Previous studies have shown that protocatechuic acid has an amazing antioxidant property. Free radicals, including 2,2-azino-bis(3-ethylbenzthiazoline-6-sulfonic acid) (ABTS), 1,1-diphenyl-2-picryl-hydrazyl (DPPH), hydroxyl radical, superoxide anion radicals ($^{\cdot}O_2^-$), ferric ions (Fe^{3+}), cupric ions (Cu^{2+}), and ferrous ions (Fe^{2+}) attack lipids, carbohydrates, proteins and DNA, which leads to various disorders and diseases. Protocatechuic acid terminates these attacks through its scavenging and chelating activities.[28] Further, protocatechuic acid demonstrates other remarkable pharmacological activities such as anticancer,[29] antitumor,[30] antimutagenic,[31] antibacterial,[32] anti-inflammatory,[33] antigenotoxic,[34] cardioprotective, and chemopreventive.[35] It has been shown to cause markedly apoptotic effects in the treatment of several types of cancer cells, including human leukemia (pa-2000-leukemia), cervix, breast, lung, liver, and prostate. It induces cell death via increasing DNA fragmentation, decreasing mitochondrial membrane potential, lowering Na-K-ATPase activity, and elevating caspase-3 and caspase-8 activities in cancerous cells. Moreover, protocatechuic acid inhibits cell adhesion and the production of vascular endothelial growth factor, interleukin (IL) 6, IL-8, and intercellular adhesion molecule 1 in cancer cells and does not have negative effects on normal human cells.[29]

However, there has been limited research undertaken on the intercalation of protocatechuic acid into LDHs. Thus, in this study, protocatechuic acid was selected as a model for an anticancer drug and was intercalated into an Mg/Al-LDH matrix using both ion-exchange and direct coprecipitation techniques. We focused our study on the spatial orientation of the protocatechuic acid anion between the layers and its thermal stability, physico-chemical features, and release properties at different pH values. In addition, we also investigated the effect of a protocatechuic acid-Mg/Al-LDH nanocomposite on the viability of MCF-7 human breast cancer, HeLa human cervical cancer, and normal cells to assess the delivery efficiency of Mg/Al-LDH vectors for use as drug-delivery nanovehicles.

Materials and methods

Materials

$Mg(NO_3)_2\cdot 6H_2O$ at 99% and protocatechuic acid ($C_7H_6O_4$, molecular weight 154.12 g/mol) at 97% purity were purchased from Acros Organics (Geel, Belgium). $Al(NO_3)_3\cdot 9H_2O$ and NaOH were purchased from Friendemann Schmidt (Parkwood, WA, USA). Phosphate-buffered saline

(PBS) was purchased from Sigma-Aldrich (St Louis, MO, USA). Deionized water was used in all experiments. MCF-7, HeLa, and 3T3 cell lines were obtained from the American Tissue Culture Collection (Manassas, VA, USA).

Synthesis

Synthesis of Mg/Al-NO_3 LDH

$MgAl\text{-}NO_3$was prepared using the coprecipitation method. An aqueous solution of 2 M NaOH was added dropwise to a solution (250 mL) containing a Mg^{2+} to Al^{3+} molar ratio of 4:1 under a nitrogen atmosphere with vigorous stirring until the final pH of 10 was reached. The suspension was then aged at 70°C for 18 hours. The resulting precipitate was filtered and washed with deionized water and finally dried in an oven at 60°C.

Synthesis of protocatechuic acid-Mg/Al nanocomposite using the ion-exchange method

The protocatechuic acid-intercalated $Mg/Al\text{-}NO_3$ was prepared using the ion-exchange method. Protocatechuic acid (1.6 g, 0.2 M) was dissolved in 50 mL water and added to the aqueous solution containing 0.2 g $Mg/Al\text{-}NO_3$. The pH of the reaction mixture was kept at 10 by the simultaneous addition of 2 M NaOH solution and the mixture was stirred vigorously for 2 hours at room temperature. The reaction mixture was aged at 70°C for 18 hours before the resulting slurry was centrifuged, washed with water, and dried in an oven at 60°C. The product was labeled "PANE" (ie, protocatechuic acid-Mg/Al nanocomposite synthesized using the ion-exchange method).

Synthesis of protocatechuic acid-Mg/Al nanocomposite using the direct method

Protocatechuic acid was intercalated into Mg/Al-LDH using the direct coprecipitation method. An aqueous solution of protocatechuic acid (1.6 g, 0.2 M) and 2 M NaOH was added dropwise into a solution (250 mL) containing Mg^{2+} and Al^{3+} nitrate at a molar ratio of 4:1 under a nitrogen atmosphere with vigorous stirring. The final pH of the solution was adjusted to 10. The suspension was aged at 70°C for 18 hours and the resulting precipitate was filtered, washed with water, and dried in an oven at 60°C. The product was labeled "PAND" (ie, protocatechuic acid-Mg/Al nanocomposite synthesized using the direct method).

Characterization

Powder X-ray diffraction (XRD) patterns were recorded in the range of 2°–60° on a Shimadzu XRD-6000 Diffractometer (Kyoto, Japan) using CuK_α radiation ($\lambda = 1.5418$ Å) at 30 kV and 30 mA. Fourier transform infrared (FT-IR) spectra of the materials were recorded over the range of 400–4000 cm^{-1} on a PerkinElmer 1752 Spectrophotometer (Waltham, MA, USA) using the KBr disc method with a 1% sample in 200 mg of spectroscopic-grade KBr, with the pellets made by pressing at 10 tons. The carbon, hydrogen, and nitrogen contents of the nanocomposites were analyzed on a Leco CHNS-932 elemental analyzer (St Joseph, MI, USA). Inductively coupled plasma-atomic emission spectrometry using a Perkin-Elmer Optima 2000DV spectrophotometer under standard conditions was used to determine the Mg to Al ratio of the chemical composition of the samples. Thermogravimetric and differential thermogravimetric analyses were carried out using a Mettler Toledo TGA/SBTP 851^e (Greifensee, Switzerland) under a nitrogen atmosphere (with an N_2 flow rate of 50 mL/minute) and a heating rate of 10°C/minute, in the range of 20°C–1000°C. Surface characterization of the material was carried out using the nitrogen gas adsorption–desorption technique at 77 K, using a Micromeritics ASAP 2000 (Norcross, GA, USA). The surface morphology of the samples was observed by a scanning electron microscope (Nova™ NanoSEM 230 model, FEI, Hillsboro, OR, USA). A PerkinElmer Lambda 35 ultraviolet–visible spectrophotometer was used to measure optical and controlled-release properties of the samples.

Controlled-release study

The protocatechuic acid release profiles were determined using PBS solutions of pH 4.8, 5.3 and 7.4 by adding 71.5 mg of PANE or PAND to 500 mL of the buffer solutions. The cumulative amount of protocatechuic acid released into the solutions was measured at predetermined time intervals using the ultraviolet–visible spectrophotometer at 255.8 nm. To compare the release rate of protocatechuic acid from Mg/Al-LDH with that of the physical mixture of protocatechuic acid and pristine Mg/Al-LDH, 0.49 mg of a physical mixture of protocatechuic acid (0.13 mg) and pristine Mg/Al-LDH (0.36 mg) was used to perform the same protocatechuic acid release experiments as already described.

Cell culture

MCF-7, HeLa, and 3T3 cell lines were maintained in Roswell Park Memorial Institute (RPMI) 1640 medium, supplemented with 10% fetal bovine serum, L-glutamine 15 mM, penicillin 100 µg mL, and streptomycin 100 µg/mL, and incubated at 37°C in humidified 5% CO_2.

Cytotoxicity assay using 3-(4, 5-dimethylthiazol-2-yl)-2,5-diphenyltetrazolium bromide (MTT) was performed by plating the cells into a 96-well plate at a density of 1.0×10^5 cells/well in 100 µL of cell culture medium and allowing to attach overnight. PANE and PAND and protocatechuic acid stock solution were prepared in dimethyl sulfoxide (DMSO), and subsequently diluted in culture medium to dilute to the various concentrations of 1.562–50.000 µg/mL and give a final volume of 200 µL in each well. Cell viability was assessed using an MTT solution after exposure to the nanocomposites and protocatechuic acid. After 72 hours exposure time, a 20 µL aliquot of the MTT solution at a concentration of 5 mg/mL was added to each well and incubated at 37°C for 4 hours. To solubilize the formazan after 4 hours of incubation, 100 µL of DMSO was added to each well and the plates were kept in a dark place within a shaker at room temperature for 30 minutes. Absorbance of the test solution in the 96-well plates was measured at 570 nm using a microplate reader. Presented cell cytotoxicity data are expressed as the percentage of cell viability compared with untreated cells under the same experimental conditions.

Results and discussion

Powder X-ray diffraction

Figure 1 illustrates the powder XRD patterns of the pristine LDH, PANE and PAND, and free protocatechuic acid. The two intense lines at a low 2θ angle of 11.09° and 22.21° in the powder XRD pattern of the pristine Mg/Al-LDH sample (Figure 1A), which was used for preparation of PANE, correspond to diffractions by planes 003 and 006, respectively, with a basal spacing value of 7.9 and 3.9 Å, respectively.[36] The interlayer distance (d_{003}) value of the pristine LDH sample (Figure 1A) is 7.9 Å, clearly lower than 8.2 Å. This is due to the low nitrate anions that lie in the center of the interlayer galleries.[37]

For PANE, a new diffraction pattern at $d_{003} = 8.3$ Å appears (Figure 1B), whereas for PAND a new diffraction pattern at $d_{003} = 9.5$ Å appears (Figure 1C). The change in the 003 basal reflection pattern of PANE and PAND compared with the pristine Mg/Al-LDH sample indicates the successful intercalation of protocatechuic acid into the nanocomposites.

The slight discrepancy in the d_{003} different value between PANE and PAND is probably due to the content of water in the interlayer galleries and different charge density of the layers.[38]

Spatial orientation of the protocatechuic acid intercalated into PANE and PAND

Figure 2A shows the molecular size dimensions of protocatechuic acid estimated by ChemOffice software (Cambridge, MA, USA). From the XRD patterns, we determined that the d spacing (d_{003}) of PANE was 8.3 Å (obtained by averaging the higher two-order peaks) and 9.0 Å (obtained by averaging the higher three-order peaks) for PAND. The thickness of the brucite-like layer of Mg/Al-LDH is 4.8 Å.[39] Therefore, the gallery height of the LDH after the intercalation of protocatechuic acid could be calculated by the d spacing minus the thickness of the LDH layer, which were 3.5 Å (8.3–4.8 Å) and 4.2 Å (9.0–4.8 Å) for PANE and PAND, respectively. The three axes of protocatechuic acid were 9.0 Å, 6.8 Å, and 2.9 Å, for the x-, y-, and z-axis, respectively.

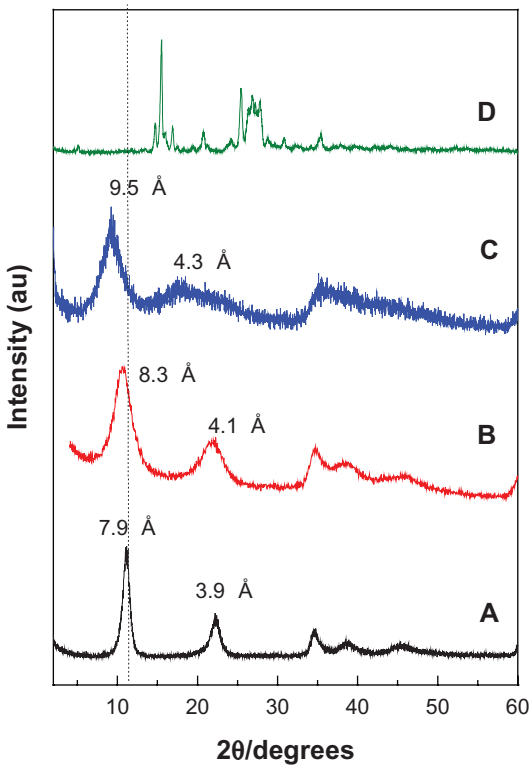

Figure 1 Powder X-ray diffraction patterns for the Mg/Al-layered double hydroxide (**A**), PANE (**B**), PAND (**C**), and free protocatechuic acid (**D**).
Abbreviations: PAND, protocatechuic acid-Mg/Al nanocomposite synthesized by direct method; PANE, protocatechuic acid-Mg/Al nanocomposite synthesized by ion-exchange method.

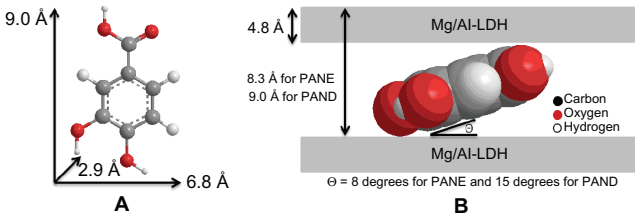

Figure 2 Three-dimensional structure of protocatechuic acid (**A**) and molecular structural models of PANE and PAND, protocatechaic acid intercalated between interlayers of Mg/Al-layered double hydroxide (**B**).
Abbreviations: PAND, protocatechuic acid-Mg/Al nanocomposite synthesized by direct method; PANE, protocatechuic acid-Mg/Al nanocomposite synthesized by ion-exchange method; LDH, layered double hydroxide.

The gallery height of the nanocomposites were 3.5 and 4.2 Å for PANE and PAND, respectively, both of which are much smaller than the value of the long and short axes (9.0 and 6.8 Å, respectively) and slightly larger than the thickness of protocatechuic acid (2.9 Å). This suggests that the protocatechuic acid anions in PANE and PAND were accommodated as a monolayer in each nanocomposite with an angle from the z-axis of 8° in PANE and 15° in PAND, as shown in Figure 2B.

Infrared spectroscopy

The Fourier transform infrared (FTIR) spectra of protocatechuic acid, Mg/Al-LDH, PANE, and PAND are shown in Figure 3. The FTIR spectrum of Mg/Al-LDH (Figure 3B) shows a strong absorption band at 1385 cm^{-1} that can be attributed to the stretching vibration of NO_3^-.[40] In the low-frequency region, the absorption peaks indicate that the lattice vibration modes can be attributed to M–O and O–M–O at 610 and 837 cm^{-1}, respectively.[41] In the FTIR spectrum of pristine protocatechuic acid (Figure 3A), there is a stretching vibration band for the OH group at 3202 cm^{-1}. A band due to C–H in the plane bending of the aromatic ring was recorded at 1098 cm^{-1}. Bands between 1526 cm^{-1} and 1416 cm^{-1} and at 1599 cm^{-1} can be attributed to C–C stretching for the benzene ring. The strong band at 1664 cm^{-1} can be attributed to the stretching of the C=O group of the carboxylic group and the band at 931 cm^{-1} is due to the O–H bending for the carboxylic group. The FTIR spectra of PANE and PAND are shown in Figure 3C and D, respectively. The characteristic C–O stretching vibration of the carboxylic group at 1664 cm^{-1} can be seen to have vanished from the FTIR of the nanocomposites. At the same time, intense peaks at 1507 and 1364 cm^{-1} for PANE and 1506 and 1367cm^{-1} for PAND are due to asymmetric and symmetric stretching, respectively, of the COO– group can be clearly observed.[42] The band at 550 cm^{-1} and at 566 cm^{-1} for PANE and PAND, respectively, can be attributed to M–O and O–M–O, respectively.

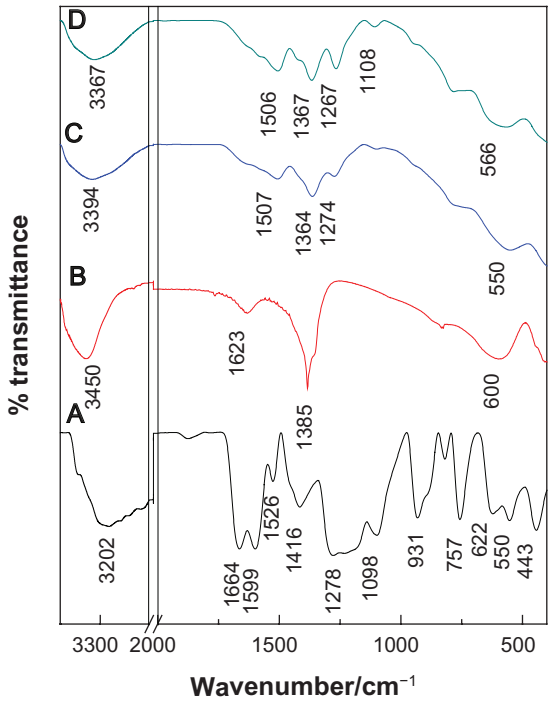

Figure 3 Fourier transform infrared spectra of free protocatechuic acid (**A**) Mg/Al-layered double hydroxide (**B**), PANE (**C**), and PAND (**D**).
Abbreviations: PAND, protocatechuic acid-Mg/Al nanocomposite synthesized by direct method; PANE, protocatechuic acid-Mg/Al nanocomposite synthesized by ion-exchange method.

Elemental analysis

The carbon, hydrogen, nitrogen and sulphur (CHNS) analysis and inductively coupled plasma elemental data were used to determine the drug and inorganic layer compositions of PANE and PAND. As shown in Table 1, PANE and PAND contained both drug and inorganic layers, indicating that both of these were constituents of the nanocomposites. This shows that protocatechuic acid was intercalated into the Mg/Al-LDH inorganic interlayers. Table 1 shows that the Mg^{2+} to Al^{3+} molar ratio in PANE and PAND was 3.3 and 2.9, respectively, compared with the initial molar ratio of 4.0. As a result of the elemental chemical analysis and thermogravimetric studies, the empirical formula for PANE was determined to be $[Mg_{0.77}Al_{0.23}(OH)_2](PA^-)_{0.177}(NO_3^-)_{0.053}\cdot yH_2O$, while it was $[Mg_{0.74}Al_{0.26}(OH)_2](PA^-)_{0.209}(NO_3^-)_{0.051}\cdot yH_2O$ for PAND.

Thermal analysis

Results of thermal analysis of pure protocatechuic acid, PANE, and PAND are shown in Figure 4A–C, respectively. For protocatechuic acid (Figure 4A), four thermal events were clearly observed. The first event, which occurred in the region of 55°C–129°C, was attributed to the removal of absorbed water molecules, corresponding to a sharp peak in the differential thermogravimetric curve at 101°C, with a weight loss of 2.9%. This was followed by a second stage at 175°C–299°C due to the decomposition combustion of protocatechuic acid, which corresponded to a strong peak at 250°C and a weight loss of 79.4%. The third and fourth weight losses occurred in the region of 299°C–408°C and 408°C–593°C, respectively, with 6.4% and 12.2% weight loss, respectively.

Figure 4B and C show the thermal decomposition of PANE and PAND, respectively. As shown in the figure, it

Table 1 Elemental chemical composition for protocatechuic acid and its nanocomposites

Sample	C[a] (%w/w)	N[a] (%w/w)	Mg[b] (%w/w)	Al[b] (%w/w)	X[b]	Anion[a] (%w/w)	Mg/Al[b]	Empirical formula[b]
PANE	13.37	0.676	19.1	6.1	0.23	24.5	3.3	$[Mg_{0.77}Al_{0.23}(OH)_2](PA^-)_{0.177}(NO_3^-)_{0.053}\cdot yH_2O$
PAND	14.98	0.607	17.3	6.7	0.26	27.5	2.9	$[Mg_{0.74}Al_{0.26}(OH)_2](PA^-)_{0.209}(NO_3^-)_{0.051}\cdot yH_2O$

Notes: [a]Estimated from CHNS analysis; [b]estimated from inductively coupled plasma analysis.
Abbreviations: C, carbon; N, nitrogen; Mg, magnesium; Al, aluminum; X, aluminum mole fraction; Y, the mole of water molecules; PAND, protocatechuic acid-Mg/Al nanocomposite synthesized by direct method; PANE, protocatechuic acid-Mg/Al nanocomposite synthesized by ion-exchange method; CHNS, carbon, hydrogen, nitrogen, sulphur.

progressed through two major stages of weight loss; these occurred at temperature maxima of 93°C and 115°C, and 462°C and 500°C, with weight losses of 20.1% and 15.2%, and 34.8% and 40.7% for PANE and PAND, respectively. The first stage of weight loss in the range 39°C–270°C was due to the removal of water physisorbed on the external surface of the LDH as well as structured water. The second weight loss in the range 277°C–642°C and 262°C–997°C, with a total weight loss of 34.8% and 40.7%, for PANE and PAND, respectively, can be attributed to de-hydroxylation of the metal hydroxide layers and decomposition of nitrate ions.

Decomposition of protocatechuic acid in PANE and PAND occurred at 462°C and 500°C, respectively, both of which are higher temperatures than that for the decomposition of the free protocatechuic acid (250°C). This suggests that the thermal stability of protocatechuic acid in the nanocomposites was enhanced due to the intercalation process as a result of the electrostatic attraction between the negatively charged carboxylate group of the protocat-

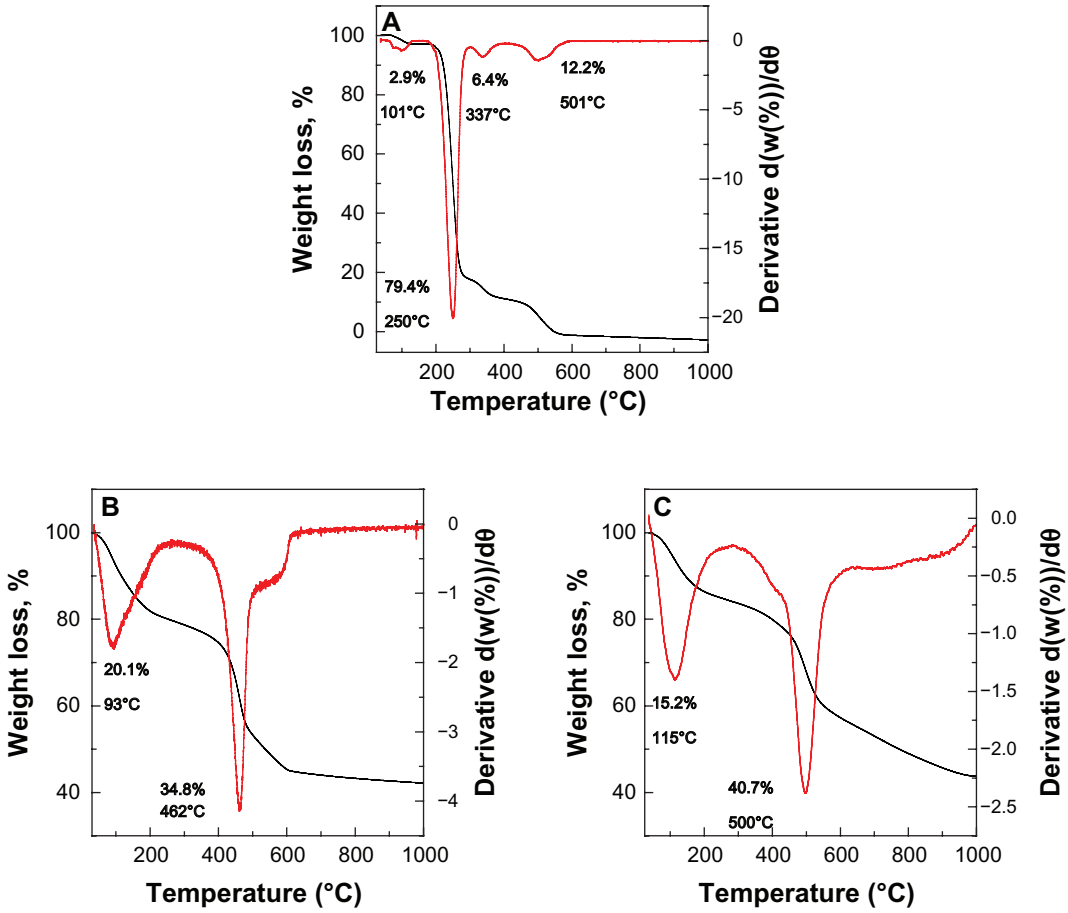

Figure 4 Thermogravimetric and differential thermogravimetric thermograms of protocatechuic acid (**A**), PANE (**B**), and PAND (**C**).
Note: The black line is the thermogravimetric analysis.
Abbreviations: PAND, protocatechuic acid-Mg/Al nanocomposite synthesized by direct method; PANE, protocatechuic acid-Mg/Al nanocomposite synthesized by ion-exchange method.

echuic acid and the positively charged brucite-like layers of Mg/Al-LDH.

Surface properties

The surface morphologies of Mg/Al-LDH, PANE, and PAND are shown in Figure 5. The micrographs in Figure 5 were obtained using a field-emission scanning electron microscope (Figure 5A and D at 10,000×; Figure 5B, E, and G, at 25,000×; and Figure 5C, F, and H at 50,000 × magnification). As shown in this figure, all samples had typical, nonuniform, irregular agglomerates of compact and nonporous plate-like structures.

Figure 6A shows the adsorption–desorption isotherms for Mg/Al-LDH, PANE, and PAND. As shown in the figure, all isotherms are Type IV (according to the International Union of Pure and Applied Chemistry classification), indicating a mesopore-type material.[43] It can be seen that the adsorbate uptake of Mg/Al-LDH was slow at the relative pressure range of 0.0–0.4, but rapid adsorption was observed after this, with an optimum uptake of about 18 cm^3/g, indicating a high capacity for nitrogen gas uptake. However, for PANE and PAND, the uptake was slow until a relative pressure of 0.8 was reached. Further increase in the relative pressure beyond 0.8 resulted in rapid adsorption of the absorbent and an optimum uptake of 9.0 cm^3/g and 3.0 cm^3/g for PANE and PAND, respectively. The desorption branch of the hysteresis loop for Mg/Al-LDH was different from that of PANE and PAND. PANE displayed an H1-type branch (open-ended cylindrical pore), while PAND was found to have an H2-type branch (with open slit-shaped capillaries).[44] As a result of nitrogen adsorption, the surface area of the materials determined using the Brunauer, Emmet, and Teller (BET) method decreased from 9 m^2/g for Mg/Al-LDH to 3 and 2 m^2/g for PANE and PAND, respectively. This was due to the change in the porous texture as a result of the formation of the nanocomposite compounds.

Figure 6B shows plots of the Barret–Joyner–Halenda (BJH) desorption pore size distribution for Mg/Al-LDH, PANE, and PAND. As shown in the figure, a single-peaked pore size distribution was observed for Mg/Al-LDH, centered at around 60 Å. In contrast, a single peak each for PANE and PAND appears at 88 and 43 Å, respectively. Due to the intercalation process, the BJH pore volume decreased from 0.03 for Mg/Al-LDH to 0.01 cm^3/g for PANE and PAND,

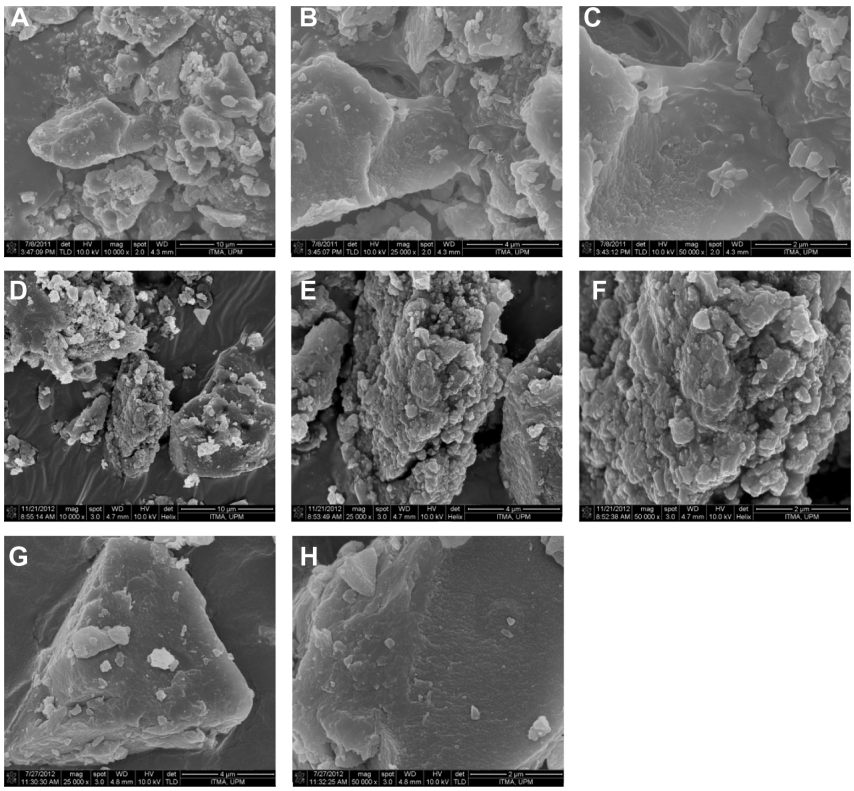

Figure 5 Field-emission scanning electron micrographs of: Mg/Al-layered double hydroxide at (**A**) 10,000×, (**B**) 25,000×, and (**C**) 50,000 × magnification; PANE at (**D**) 10,000×, (**E**) 25,000×, and (**F**) 50,000 × magnification; and PAND nanocomposite (**G**) 25,000× and (**H**) 50,000 × magnification.
Abbreviations: PAND, protocatechuic acid-Mg/Al nanocomposite synthesized by direct method; PANE, protocatechuic acid-Mg/Al nanocomposite synthesized by ion-exchange method.

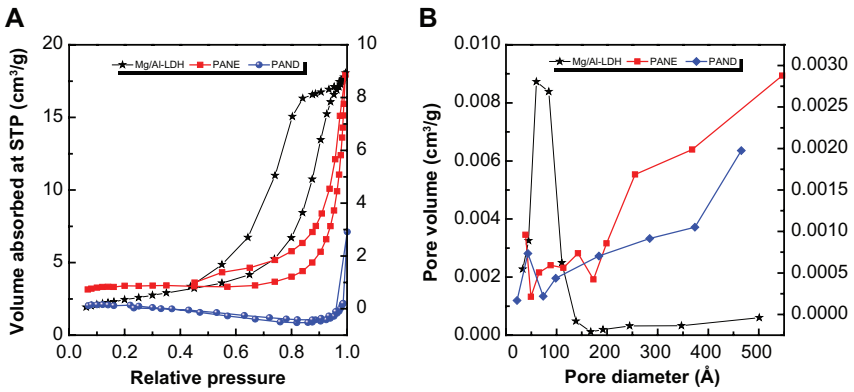

Figure 6 Adsorption–desorption isotherms (**A**) and BJH pore size distribution (**B**) for Mg/Al-LDH, PANE, and PAND.
Abbreviations: BJH, Barret–Joyner–Halenda (method); LDH, layered double hydroxide; PAND, protocatechuic acid-Mg/Al nanocomposite synthesized by direct method; PANE, protocatechuic acid-Mg/Al nanocomposite synthesized by ion-exchange method; STP, standard temperature and pressure.

whereas the BJH average pore diameter increased from 65 Å for Mg/Al-LDH to 147 and 152 Å for PANE and PAND, respectively (Table 2).

Release behavior of protocatechuic acid from PANE and PAND

The release profiles of protocatechuic acid from the nanocomposites and the physical mixture of protocatechuic acid and pristine Mg/Al-LDH are shown in Figure 7. The physical mixture of protocatechuic acid and pristine Mg/Al-LDH exposed to pH 4.8 and pH 7.4 environments show the release of protocatechuic acid very quickly, within 10 minutes (Figure 7A). In contrast, the release rate of protocatechuic acid from PANE and PAND was slower than from the physical mixture, indicating that PANE and PAND have the potential to be used for the controlled release of drugs. This result may be attributed to the interaction between the negatively charged protocatechuic acid and the positively charged inorganic LDH layers.

In addition, the release rate of protocatechuic acid from PANE and PAND was dependent on the pH of the environment. The release rate at pH 7.4 was markedly lower than that at pH 5.3 and 4.8 for both nanocomposites.

Table 2 Surface properties of Mg/Al-layered double hydroxide (LDH) and its nanocomposites, PANE and PAND

Sample	BET surface area, m^2/g	BJH pore volume, cm^3/g	BJH average pore diameter, Å
Mg/Al-LDH	9	0.027	65
PANE	3	0.011	147
PAND	4	0.011	152

Abbreviations: BET, Brunauer, Emmet, and Teller (method); BJH, Barret–Joyner–Halenda (method); PAND, protocatechuic acid-Mg/Al nanocomposite synthesized by direct method; PANE, protocatechuic acid-Mg/Al nanocomposite synthesized by ion-exchange method.

In Figure 7B, the percent release of protocatechuic acid from PANE can be seen to have reached about 85% within about 1000 minutes when exposed to a pH of 4.8 and to have reached 82% by 3894 minutes at a pH of 5.3. About 59% of release had occurred within about 7500 minutes when exposed to a pH 7.4 environment. Figure 7C shows that the release profile of the drug from PAND reached about 98% and 83% when exposed to pH 4.8 and 7.4 within 900 and 4000 minutes, respectively. About 87% of the drug was released within about 1349 minutes when exposed to a pH 5.3 environment. The difference in release rates at pH 4.8, 5.3, and 7.4 may be due to a difference in release mechanism between protocatechuic acid and the nanocomposites. At acidic pH (4.8 or 5.3), LDHs are unstable and can easily dissolve,[45] therefore drug release can occur if the LDH interlayers are removed. At pH 7.4, LDHs are more stable compared with at pH 4.8 or 5.3 and, as a result, the release would occur primarily through the ion exchange between the protocatechuic acid and the negative anions available in the PBS.

Release kinetics of protocatechuic acid from PANE and PAND

There are various kinetic models that can be used to describe the total release of drugs from the interlayers of nanocomposites. Common models used include pseudo-first order, pseudo-second order, and parabolic diffusion. The pseudo-first order kinetic equation is:

$$\ln (q_e - q_t) = \ln q_e - k_1 t,$$

where "q_e" and "q_t" are the equilibrium release amount and the release amount at time t, respectively, and "k_1" is the corresponding release rate constant. A plot between $\ln (q_e - q_t)$

Table 3 Correlation coefficient (R^2) and rate constant (k) obtained by fitting the data of the release of protocatechuic acid from PANE and PAND nanocomposites into phosphate-buffered saline solution at pH 4.8, 5.3, and 7.4

Samples	pH	Saturation release (%)	R^2			Pseudo-second order[a]	Pseudo-first order[b]	Parabolic diffusion[c]
			Pseudo-first order	Pseudo-second order	Parabolic diffusion	Rate constant, k (mg/min)	Rate constant, k (min^{-1})	Rate constant, k (min^{-1})
PANE	7.4	59	0.9804	0.9989[a]	0.8860	2.2×10^{-5}	–	–
PANE	5.3	82	0.9147[c]	0.8469	0.8517		4.9×10^{-4}	–
PANE	4.8	85	0.9060	0.9601[a]	0.8334	4.1×10^{-5}	–	–
PAND	7.4	83	0.9848	0.9910[a]	0.8266	2.3×10^{-5}	–	–
PAND	5.3	87	0.9543	0.9652	0.9796[c]		–	3.1×10^{-2}
PAND	4.8	98	0.9805[b]	0.8272	0.9563	–	2.1×10^{-3}	–

Notes: [a]Rate release constant for pseudo-second order; [b]rate release constant for pseudo-first order; [c]rate release constant for parabolic diffusion.
Abbreviations: PAND, protocatechuic acid-Mg/Al nanocomposite synthesized by direct method; PANE, protocatechuic acid-Mg/Al nanocomposite synthesized by ion-exchange method.

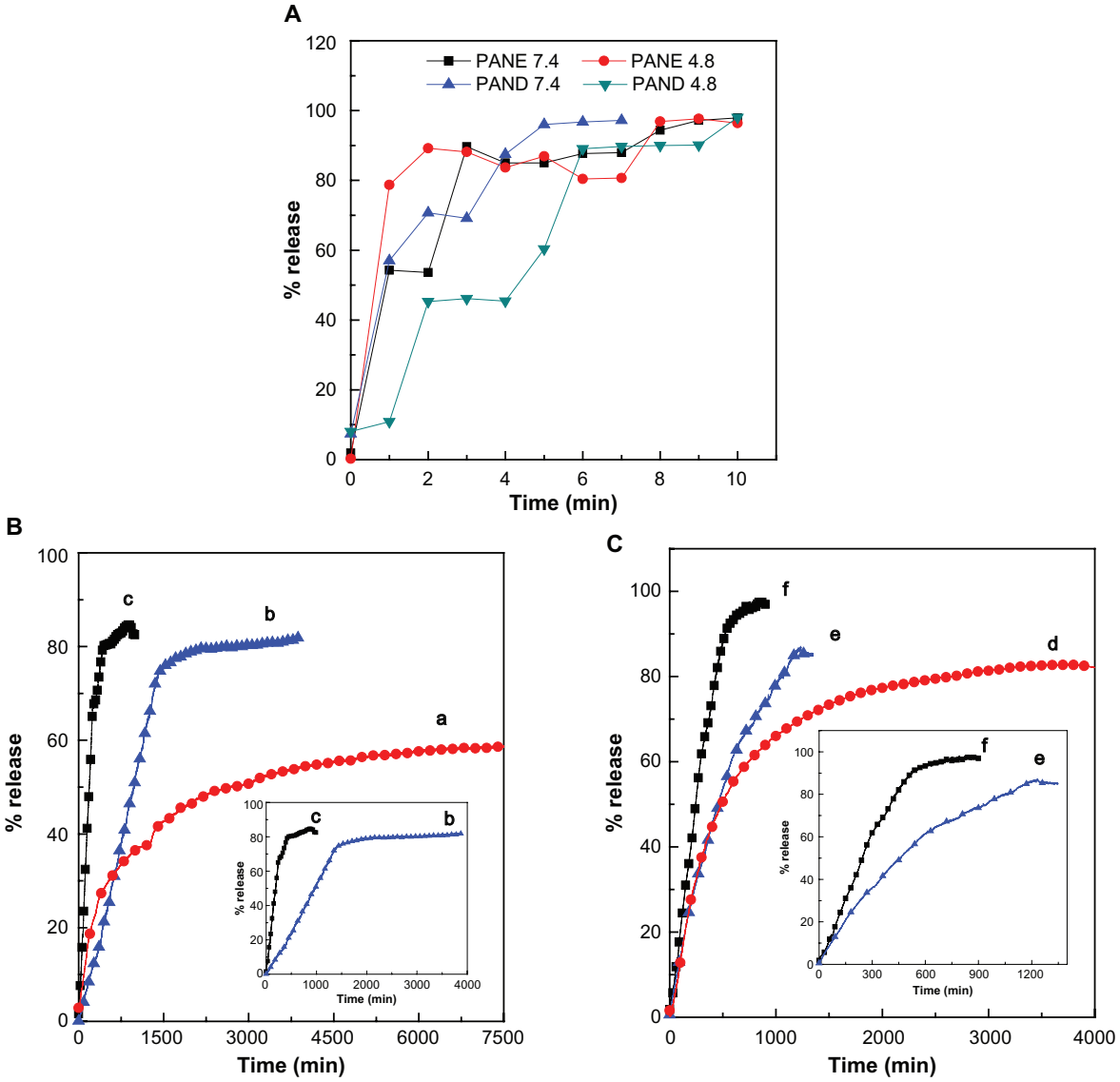

Figure 7 (**A**) Release profiles of physical mixture of protocatechuic acid with Mg/Al-layered double hydroxide. (**B**) Release profiles of protocatechuic acid from PANE at pH 7.4 (**a**), pH 5.3 (**b**), and pH 4.8 (**c**). (**C**) Release profiles of protocatechuic acid from PAND at pH 7.4 (**d**), pH 5.3 (**e**), and pH 4.8 (**f**). Insets show the release details.
Abbreviations: PAND, protocatechuic acid-Mg/Al nanocomposite synthesized by direct method; PANE, protocatechuic acid-Mg/Al nanocomposite synthesized by ion-exchange method.

against time, t, gives a straight line and the rate constant value can be calculated.

In the pseudo-second order kinetic model, the release behavior of drugs from a nanocomposite can be described as:[46]

$$t/q_t = 1/k_2 q_e^2 + t/q_e$$

By plotting t/q_t against t, a straight line is obtained and the rate constant, k_2, as well as q_e can be calculated using the relation:

$$k_2 = 1/q_e^2 \cdot \text{intercept}$$

The parabolic diffusion kinetic model can be written as:[47]

$$1-(M_t/M_o)/t = k_3 t^{-0.5} + b,$$

where "M_o" and "M_t" are the drug content remaining in the LDH at release time 0 and t, respectively, "k_3" is the corresponding release rate constant, and b is a constant.

Using the above three kinetic models, it was found that the pseudo-second order model was more satisfactory for describing the release kinetic processes of protocatechuic acid from PANE at pH 7.4 and 4.8 and from PAND at pH 7.4, with a coefficient of determination (R^2) of 0.9989, 0.9601,

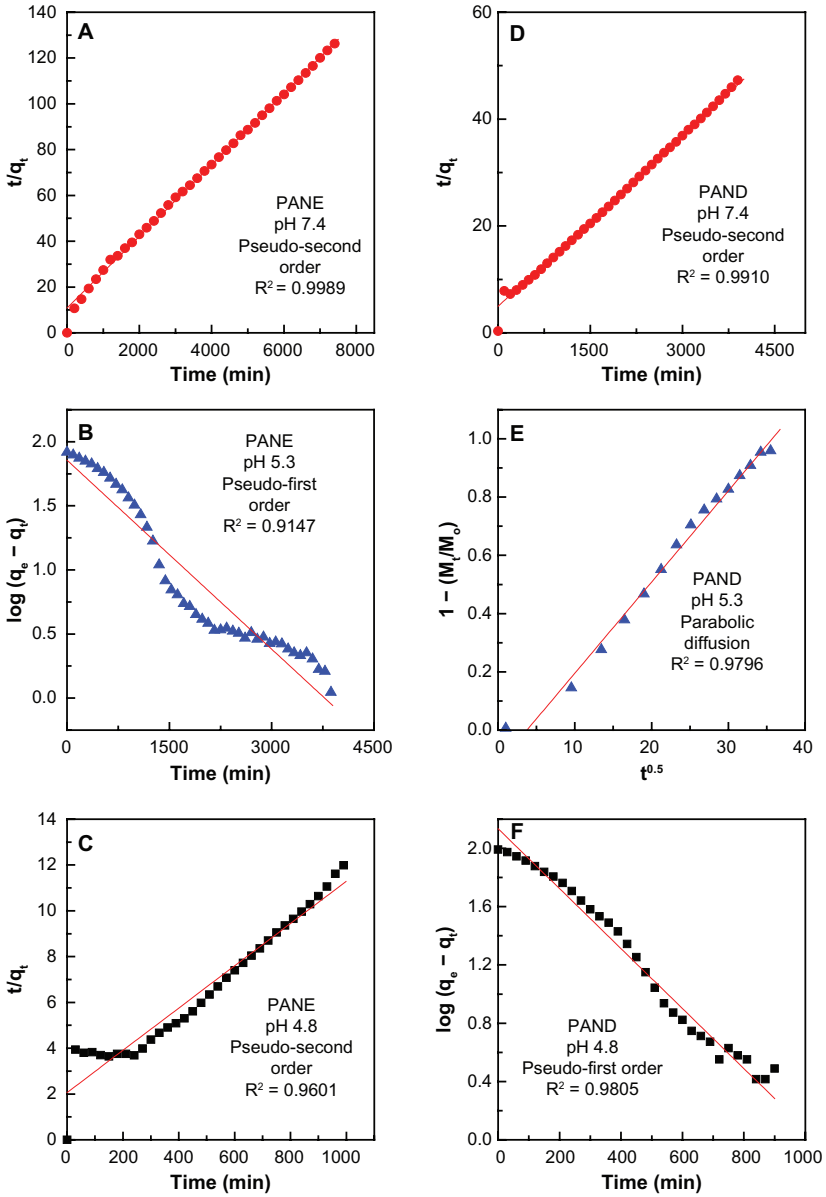

Figure 8 Fitted data for the release of protocatechuic acid from PANE samples at (**A**) pH 7.4, (**B**) 5.3, and (**C**) 4.8 and from PAND samples at (**D**) pH 7.4, (**E**) 5.3, and (**F**) 4.8.
Abbreviations: PAND, protocatechuic acid-Mg/Al nanocomposite synthesized by direct method; PANE, protocatechuic acid-Mg/Al nanocomposite synthesized by ion-exchange method; min, minute.

and 0.9910, respectively (Figure 8 and Table 3). The release of protocatechuic acid from PAND at pH 4.8 obeyed the pseudo-first order kinetic model, with $R^2 = 0.9805$ (Table 3). The release kinetic process of protocatechuic acid from PANE and PAND in a pH 5.8 environment obeyed the pseudo-first order and parabolic diffusion model, respectively, with an R^2 of 0.9147 and 0.9796, respectively.

For PANE (Table 3), the rate release constant (k) value was 2.2×10^{-5} and 4.1×10^{-5} mg/min at pH 7.4 and 4.8, respectively, and for PAND the corresponding value was 2.3×10^{-5} mg/min at pH 7.4 (pseudo-second order) and 2.1×10^{-3} min^{-1} at pH 4.8 (pseudo-first order). The rate constant for pseudo-first order at pH 5.3 was 4.9×10^{-4} min^{-1}, while for the parabolic diffusion model it was 3.1×10^{-2} min^{-1}.

Cytotoxicity assay of protocatechuic acid, PANE, and PAND samples against 3T3, HeLa, and MCF-7 cell lines

The beneficial efficiency of PANE and PAND compared with free protocatechuic acid was investigated by cytotoxicity assay using two cancer cells, the HeLa cervical cancer cell line and the MCF-7 breast cancer cell line. In addition, the 3T3 cell line of normal fibroblast cells was used to evaluate drug-induced toxicity. Figure 9A shows that protocatechuic acid, PANE, and PAND did not show any toxic effects against normal fibroblasts. Figure 9B and C show the dose-dependent cell viability of HeLa and MCF-7 cells, respectively. Overall, the protocatechuic acid, PANE, and PAND gradually suppressed the tumor cell growth in a dose-dependent manner.

Figure 9B and Table 4 clearly show that the tumor suppression (cytotoxicity) efficiency can be described in the following order: PANE > PAND > protocatechuic acid in HeLa cells, with half maximal inhibitory concentration values of 19.8, 30.3, and 38.4 μg/mL, respectively. Figure 9C and Table 4 indicate that protocatechuic acid did not show any significant cytotoxicity against MCF-7 cells, and that PANE had a higher tumor suppression efficiency than PAND, with half maximal inhibitory concentration values of 35.6 and 36.0 μg/mL, respectively.

Figure 9B shows that when the concentration was increased from 1.562 to 50.000 μg/mL, there was a rapid decrease in cell viability. The maximum suppression effects of protocatechuic acid, PANE, and PAND were observed at the concentration of 50 μg/mL, with 44.8%, 14.8%, and 14.3% cell viability, respectively. For MCF-7 cells, the corresponding value for protocatechuic acid, PANE, and PAND at 50 μg/mL was 50.3%, 20.6%, and 41.8%, respectively.

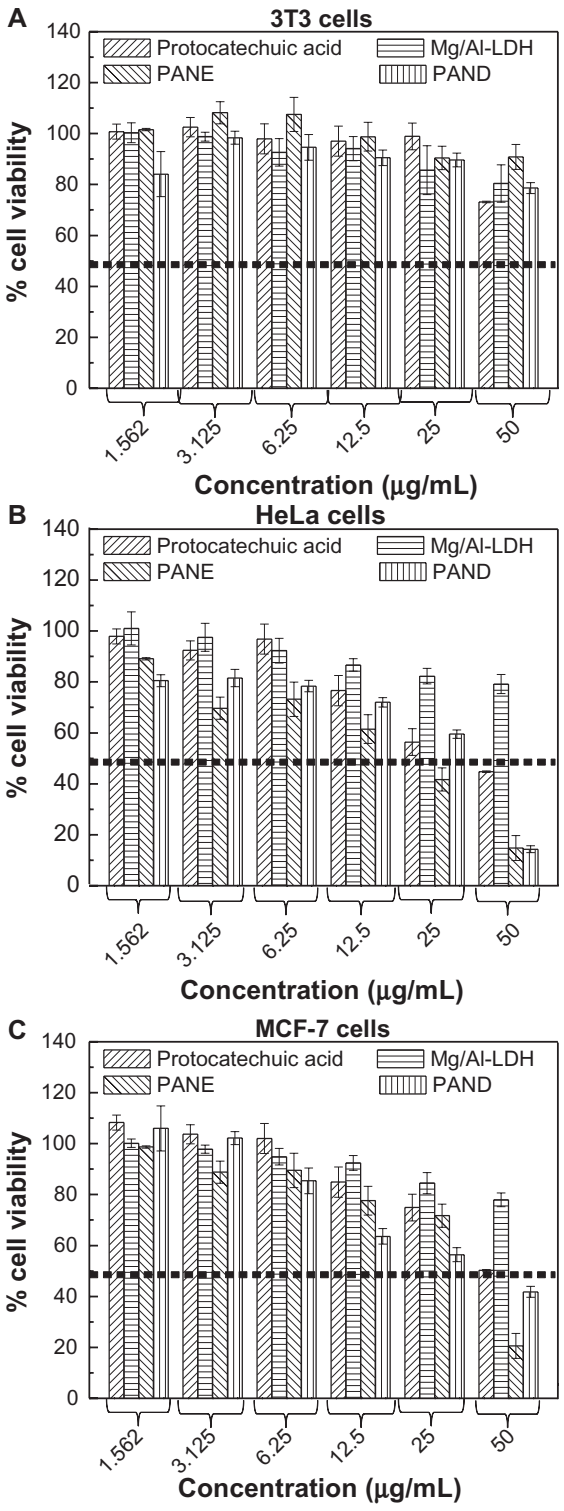

Figure 9 Cell viability (3-(4,5-Dimethylthiazol-2-yl)-2,5-diphenyltetrazolium bromide [MTT] assay) of (**A**) 3T3, (**B**) HeLa, and (**C**) MCF-7 cell lines exposed to various gradient concentrations of protocatechuic acid, Mg/Al-LDH, PANE, and PAND.

Note: Data presented are mean ± standard deviation for experiments done in triplicate.

Abbreviations: LDH, layered double hydroxide; PAND, protocatechuic acid-Mg/Al nanocomposite synthesized by direct method; PANE, protocatechuic acid-Mg/Al nanocomposite synthesized by ion-exchange method; 3T3, fibroblast cell; MCF-7, human breast cancer cell; HeLa, human cervical cancer cell.

Table 4 The half maximal inhibitory concentration (IC_{50}) values for protocatechuic acid, PANE, and PAND samples against 3T3, HeLa, and MCF-7 cell lines

Cell type	3T3			HeLa			MCF-7		
Sample	Free drug	PANE	PAND	Free drug	PANE	PAND	Free drug	PANE	PAND
IC_{50}	No cytotoxicity			38.8	19.8	30.3	–	35.6	36.0

Notes: 3T3, fibroblast cell; MCF-7, human breast cancer cell; HeLa, human cervical cancer cell.
Abbreviations: PAND, protocatechuic acid-Mg/Al nanocomposite synthesized by direct method; PANE, protocatechuic acid-Mg/Al nanocomposite synthesized by ion-exchange method.

Conclusion

In the study reported here, protocatechuic acid, an active anticancer drug, was incorporated into the Mg/Al-LDH matrix by ion-exchange and direct coprecipitation methods to form intercalated nanocomposite products. XRD and FTIR studies indicate the successful intercalation of protocatechuic acid into the inorganic inter-galleries of the LDH. Results of thermogravimetric and differential thermogravimetric analyses show that the thermal stability of the intercalated protocatechuic acid exhibited a notable increase compared with that of pristine protocatechuic acid. This finding indicates that, for PANE and PAND, the protocatechuic acid moiety was oriented as a monolayer with an angle from the z-axis of 8° in PANE and 15° in PAND. The intercalated amount of protocatechuic acid in PANE and PAND was 24.5% and 27.5% (w/w), respectively.

The in vitro protocatechuic acid release from PANE and PAND was markedly lower than that from the corresponding physical mixture of the drug with pristine LDH at pH 4.8, 5.3, and 7.4. In addition, the release rate of protocatechuic acid from the nanocomposites at pH 7.4 was markedly lower than that at pH 4.8 and 5.3, and this is due to a possible difference in the release mechanism. At pH 7.4, the mechanism possibly occurred through ion exchange, while at pH 4.8 and 5.3 it possibly occurred through both the dissolution of LDH layers and ion exchange.

Results of the in vitro cytotoxicity study indicate that the tumor suppression efficiency in HeLa and MCF-7 cells can be described in the following order: PANE > PAND > protocatechuic acid. The cytotoxicity of PANE was greater than that of PAND and this is in parallel with the higher protocatechuic acid in PANE compared with in PAND.

Acknowledgments

We would like to thank the Ministry of Science Technology and Innovation of Malaysia (MOSTI) for funding the project under grant number NND/NA/(1)/TD11-010 vot no 5489100.

Disclosure

The authors declare no conflicts of interest in this work.

References

1. Oh JM, Park M, Kim ST, Jung JY, Kang YG, Choy JH. Efficient delivery of anticancer drug MTX through MTX-LDH nanohybrid system. *J Phys Chem Solids*. 2006;67(5):1024–1027.
2. Kong X, Jin L, Wei M, Duan X. Antioxidant drugs intercalated into layered double hydroxide: structure and vitro release. *Appl Clay Sci*. 2010;49(3):324–329.
3. Yang QZ, Yang J, Zhang CK. Synthesis and properties of cordycepin intercalates of Mg-Al-nitrate layered double hydroxides. *Int J Pharm*. 2006;326(1–2):148–152.
4. Burzlaff A, Brethauer S, Kasper C, Jackisch BO, Scheper T. Flow cytometry: interesting tool for studying binding behavior of DNA on inorganic layered double hydroxide (LDH). *Cytometry A*. 2004;62(1):65–69.
5. Peterson CL, Perry DL, Masood H, et al. Characterization of antacid compounds containing both aluminum and magnesium. I. Crystalline powders. *Pharm Res*. 1993;10(7):998–1004.
6. Xu ZP, Zeng QH, Lu GQ, Yu AB. Inorganic nanoparticles as carriers for efficient cellular delivery. *Chem Eng Sci*. 2006;61(3):1027–1040.
7. Choi SJ, Oh JM, Choy JH. Human-related application and nanotoxicology of inorganic particles: complementary aspects. *J Mater Chem*. 2008;18(6):615–620.
8. Evans DG, Duan X. Preparation of layered double hydroxides and their applications as additives in polymers, as precursors to magnetic materials and in biology and medicine. *Chemical Communications*. 2006;5:485–496.
9. Desigaux L, Belkacem MB, Richard P, et al. Self-assembly and characterization of layered double hydroxide/DNA hybrids. *Nano Lett*. 2006;6(2):199–204.
10. Choy JH, Jung JS, Oh JM, et al. Layered double hydroxide as an efficient drug reservoir for folate derivatives. *Biomaterials*. 2004;25(15):3059–3064.
11. Choi SJ, Oh JM, Choy JH. Biocompatible nanoparticles intercalated with anticancer drug for target delivery: pharmacokinetic and biodistribution study. *J Nanosci Nanotechnol*. 2010;10(4):2913–2916.
12. Oh JM, Choi SJ, Lee GE, Han SH, Choy JH. Inorganic drug-delivery nanovehicle conjugated with cancer-cell-specific ligand. *Adv Funct Mater*. 2009;19(10):1617–1624.
13. Dong L, Yan L, Hou WG, Liu SJ. Synthesis and release behavior of composites of camptothecin and layered double hydroxide. *J Solid State Chem*. 2010;183(8):1811–1816.
14. Qin L, Wang S, Zhang R, Zhu R, Sun X, Yao S. Two different approaches to synthesizing Mg Al-layered double hydroxides as folic acid carriers. *J Phys Chem Solids*. 2008;69(11):2779–2784.
15. Panda HS, Srivastava R, Bahadur D. In-vitro release kinetics and stability of anticardiovascular drugs-intercalated layered double hydroxide nanohybrids. *J Phys Chem B*. 2009;113(45):15090–15100.
16. Perioli L, Posati T, Nocchetti M, Bellezza F, Costantino U, Cipiciani A. Intercalation and release of antiinflammatory drug diclofenac into nanosized ZnAl hydrotalcite-like compound. *Appl Clay Sci*. 2011;53(3):374–378.
17. Li B, He J, Evans DG, Duan X. Inorganic layered double hydroxides as a drug delivery system – intercalation and in vitro release of fenbufen. *Appl Clay Sci*. 2004;27(3):199–207.
18. Hussein Al Ali SH, Al-Qubaisi M, Hussein MZ, Ismail M, Zainal Z, Hakim MN. Controlled release and angiotensin-converting enzyme inhibition properties of an antihypertensive drug based on a perindopril erbumine-layered double hydroxide nanocomposite. *Int J Nanomedicine*. 2012;7:2129–2141.

19. Hussein Al Ali SH, Al-Qubaisi M, Hussein MZ, Ismail M, Zainal Z, Hakim MN. Comparative study of Mg/Al- and Zn/Al-layered double hydroxide-perindopril erbumine nanocomposites for inhibition of angiotensin-converting enzyme. *Int J Nanomedicine*. 2012;7:4251.
20. Hussein-Al-Ali SH, Al-Qubaisi M, Hussein MZ, Ismail M, Zainal Z, Hakim MN. In vitro inhibition of histamine release behavior of cetirizine intercalated into Zn/Al- and Mg/Al-layered double hydroxides. *Inter J Mol Sci*. 2012;13(5):5899–5916.
21. Newman SP, Jones W. Synthesis, characterization and applications of layered double hydroxides containing organic guests. *New J Chem*. 1998;22(2):105–115.
22. Rives V. *Layered Double Hydroxides: Present and Future*. New York, NY: Nova; 2001.
23. Ladewig K, Xu ZP, Lu GQ. Layered double hydroxide nanoparticles in gene and drug delivery. *Expert Opin Drug Deliv*. 2009;6(9): 907–922.
24. Tseng TH, Hsu JD, Lo MH, et al. Inhibitory effect of Hibiscus protocatechuic acid on tumor promotion in mouse skin. *Cancer Lett*. 1998;126(2):199–207.
25. Ali BH, Al Wabel N, Blunden G. Phytochemical, pharmacological and toxicological aspects of Hibiscus sabdariffa L.: a review. *Phytother Res*. 2005;19(5):369–375.
26. Jürgenliemk G, Nahrstedt A. Phenolic compounds from Hypericum perforatum. *Planta Med*. 2002;68(1):88–91.
27. Ellnain-Wojtaszek M. Phenolic acids from Ginkgo biloba L. Part II. Quantitative analysis of free and liberated by hydrolysis phenolic acids. *Acta Pol Pharm*. 1997;54(3):229–232.
28. Li X, Wang X, Chen S, Chen D. Antioxidant activity and mechanism of protocatechuic acid in vitro. *Functional Foods in Health and Disease*. 2011;7(7):232–244.
29. Yin MC, Lin CC, Wu HC, Tsao SM, Hsu CK. Apoptotic effects of protocatechuic acid in human breast, lung, liver, cervix, and prostate cancer cells: potential mechanisms of action. *J Agric Food Chem*. 2009;57(14):6468–6473.
30. Nakamura Y, Torikai K, Ohto Y, Murakami A, Tanaka T, Ohigashi H. A simple phenolic antioxidant protocatechuic acid enhances tumor promotion and oxidative stress in female ICR mouse skin: dose-and timing-dependent enhancement and involvement of bioactivation by tyrosinase. *Carcinogenesis*. 2000;21(10):1899–1907.
31. Stagos D, Kazantzoglou G, Theofanidou D, et al. Activity of grape extracts from Greek varieties of Vitis vinifera against mutagenicity induced by bleomycin and hydrogen peroxide in Salmonella typhimurium strain TA102. *Mutat Res*. 2006;609(2):165–175.
32. Liu WH, Hsu CC, Yin MC. In vitro anti-Helicobacter pylori activity of diallyl sulphides and protocatechuic acid. *Phytother Res*. 2008;22(1):53–57.
33. Liu CL, Wang JM, Chu CY, Cheng MT, Tseng TH. In vivo protective effect of protocatechuic acid on tert-butyl hydroperoxide-induced rat hepatotoxicity. *Food Chem Toxicol*. 2002;40(5):635–641.
34. Anter J, Romero-Jiménez M, Fernández-Bedmar Z, et al. Antigenotoxicity, cytotoxicity, and apoptosis induction by apigenin, bisabolol, and protocatechuic acid. *J Med Food*. 2011;14(3):276–283.
35. Tanaka T, Tanaka T, Tanaka M. Potential cancer chemopreventive activity of protocatechuic acid. *J Exp Clin Med*. 2011;3(1):27–33.
36. Jiao FP, Chen XQ, Fu ZD, Hu YH, Wang YH. Intercalation of Mg–Al layered double hydroxides by (+)-dibenzoyl-d-tartaric acid: preparation and characterization. *J Mol Struct*. 2009;921(1–3):328–332.
37. Xu ZP, Zeng HC. Decomposition pathways of hydrotalcite-like compounds $Mg_{1-x}Al_x(OH)_2(NO_3)_x \cdot nH_2O$ as a continuous function of nitrate anions. *Chem Mater*. 2001;13(12):4564–4572.
38. Wei M, Yuan Q, Evans DG, Wang Z, Duan X. Layered solids as a "molecular container" for pharmaceutical agents: L-tyrosine-intercalated layered double hydroxides. *J Mater Chem*. 2005;15(11):1197–1203.
39. Cavani F, Trifirò F, Vaccari A. Hydrotalcite-type anionic clays: preparation, properties and applications. *Catal Today*. 1991;11(2): 173–301.
40. Sun Z, Jin L, Shi W, Wei M, Duan X. Preparation of an anion dye intercalated into layered double hydroxides and its controllable luminescence properties. *Chem Eng J*. 2010;161(1–2):293–300.
41. Aisawa S, Sasaki S, Takahashi S, Hirahara H, Nakayama H, Narita E. Intercalation of amino acids and oligopeptides into Zn–Al layered double hydroxide by coprecipitation reaction. *J Phys Chem Solids*. 2006;67(5–6):920–925.
42. Ibrahim M, Nada A, Kamal DE. Density functional theory and FTIR spectroscopic study of carboxyl group. *Indian J Pure Ap Phys*. 2005;43(12):911–917.
43. Sing KS. The use of gas adsorption for the characterization of porous solids. *Colloids Surf*. 1989;38(1):113–124.
44. Pierotti RA, Rouquerol J. Reporting physisorption data for gas/solid systems with special reference to the determination of surface area and porosity. *Pure Appl Chem*. 1985;57(4):603–619.
45. Khan AI, O'Hare D. Intercalcation chemistry of layered double hydroxides: recent developments and applications. *J Mater Chem*. 2002;12:3191–3198.
46. Ho YS, Ofomaja AE. Pseudo-second-order model for lead ion sorption from aqueous solutions onto palm kernel fiber. *J Hazard Mater*. 2006;129(1–3):137–142.
47. Kong X, Shi S, Han J, Zhu F, Wei M, Duan X. Preparation of Glycyl-Tyrosine intercalated layered double hydroxide film and its in vitro release behavior. *Chem Eng J*. 2010;157(2–3):598–604.